

Static susceptibilities of dipolar ferromagnets below T_c

H. Schinz

sd&m software design & management GmbH & Co. KG, Thomas-Dehler-Straße 27, D-81737 München, Germany

F. Schwabl

Institut für Theoretische Physik, Technische Universität München, James-Frank Straße, D-85747 Garching, Germany

(Received 11 July 1997)

We study the static susceptibility tensor for the isotropic Heisenberg model with short-range nearest-neighbor exchange and long-range dipolar interactions. We derive analytic expressions for the eigenvalues and eigenvectors of the susceptibility. To this end one has to take proper account of the Goldstone modes, which lead to “critical” fluctuations at all temperatures below T_c . We discuss how the dipolar interaction modifies these effects. Instead of one longitudinal and two transverse susceptibilities in the isotropic limit, we get one longitudinal, one transverse—Goldstone-mode associated—and one intermediate susceptibility in the general dipolar case. We present a “phase diagram” exhibiting six distinct regions in the temperature–wave-vector plane. For each region we give the characteristic leading dependencies of all three susceptibilities. [S0163-1829(98)02613-7]

I. INTRODUCTION

Above the Curie temperature T_c much knowledge has been accumulated on the critical behavior of the static susceptibility of ferromagnetic materials, see, e.g., Refs. 1–4. Much work has been done on the isotropic Heisenberg model incorporating only the exchange interaction often restricted further to nearest neighbors. In real magnets, however, there inevitably exists also the dipolar interaction between the spins. Though it is small—corresponding to 10 to 100 mK while typical Curie temperatures range from 10 to 1000 K—and therefore can often be neglected, in critical phenomena it plays an important role due to the following four properties. (1) It is of long range and therefore determines the asymptotic critical properties as the correlation length diverges. (2) It is anisotropic introducing the direction of the wave vector as a preferred direction. This leads to additional angular dependencies. (3) It breaks rotation invariance, thereby lowering the symmetry, and influencing the dynamics of the order parameter markedly. (4) It introduces a second length scale in addition to the correlation length, the so-called dipolar wave vector. This leads to generalized crossover scaling laws. This second temperature-independent “mass” also suppresses fluctuations. Correspondingly, there are strong indications that the susceptibility can be described numerically quite well by a renormalized Ornstein-Zernicke form with effective exponents.^{5,4} This is partly due to the fact that the dipolar coupling does not renormalize under renormalization group transformations. Furthermore, corrections to the scaling function seem to be small.

Below T_c an additional difficulty arises from the spontaneously broken symmetry: the occurrence of Goldstone modes. These massless excitations make the system critical in the whole low-temperature phase. In low-dimensional systems these transverse fluctuations even destroy long-range order completely.⁶ In the isotropic Heisenberg model the transverse fluctuations, characterized by a $1/q^2$ divergence of the transverse susceptibility, also lead to a divergence of the

longitudinal susceptibility $\sim 1/q$ at all temperatures below T_c as the wave vector q approaches zero.^{7–15} Connected with this singularity for $q \rightarrow 0$ is a singularity of the homogeneous susceptibility ($q=0$) as an external magnetic field H approaches zero. Theoretically one expects^{16,7–9,11,14,15} a divergence $\sim H^{-1/2}$, which has meanwhile been observed experimentally by Kötzer *et al.*¹⁷

The main topic of this paper is how the dipolar interaction influences the effect of the Goldstone modes on the static susceptibilities in the ordered phase below T_c . This is of interest not only for the study of static critical phenomena itself but also enters prominently the mode-coupling equations,¹⁸ describing the dynamic critical phenomena.

An important observation is that the Goldstone fluctuations are not eliminated due to the dipolar interaction but rather their number is reduced by 1. This reduction from 2 in the isotropic case to 1 can be obtained from hydrodynamic considerations,¹¹ from spin wave theories,^{14,15} or from renormalization group theory.¹⁹ Thus, there are still Goldstone anomalies to be expected. Indeed, it can be shown that the longitudinal susceptibility still diverges $\sim 1/q$ but the amplitude is reduced by a factor of 2. This result has meanwhile also been confirmed experimentally for the strongly dipolar material EuS.¹⁷ One of the two transverse susceptibilities now diverges less rapidly ($\sim 1/q$ instead of $\sim 1/q^2$), while the other one stays as in the isotropic case ($\sim 1/q^2$), since it is associated with the one remaining Goldstone mode.

A further complication below T_c consists in the occurrence of two significant directions: the direction of the spontaneous magnetization and of the wave vector \vec{q} . This reduces the symmetry to a degree that the tensorial character of the static susceptibility has to be taken fully into account. We stress therefore the importance of a description in terms of eigenvalues and eigenvectors which has not been done in earlier treatments of this problem.

The outline of this article is as follows: In Sec. II we give a short account of a mean-field treatment of the static sus-

ceptibility, which will give some insight into the fundamental dependencies on the direction of the magnetization and the wave vector \vec{q} . In Sec. III we sketch a renormalization group treatment and derive the dominant contributions to the static susceptibility due to the fluctuations. The results are discussed in Sec. IV and the Appendix, and finally, in the fifth section, we summarize the main findings.

II. MEAN-FIELD THEORY

We start with a free-energy functional for the spin fields ϕ_q^α ($\alpha=x,y,z$):

$$\begin{aligned} \mathcal{F}(\{\phi\}) = & \int_{\vec{q}} J \left[(r+q^2) \delta^{\alpha\beta} + g \frac{q^\alpha q^\beta}{q^2} \right] \phi_q^\alpha \phi_{-\vec{q}}^\beta \\ & + \int_{\vec{q}_1} \int_{\vec{q}_2} \int_{\vec{q}_3} \sum_{\alpha,\beta} u \phi_{\vec{q}_1}^\alpha \phi_{\vec{q}_2}^\alpha \phi_{\vec{q}_3}^\beta \phi_{-\vec{q}_1-\vec{q}_2-\vec{q}_3}^\beta. \end{aligned} \quad (1)$$

Here, $r=1/\xi_+^2 \sim T-T_c$ measures the separation from T_c , J_0 and J characterize the strength of the exchange interaction while g measures the relative strength of the dipolar interaction, and u is the usual coupling constant for the quartic term. Lengths are given in units of a , the lattice constant. Thus, we can define the dipolar wave vector $q_D^2=g$.

This functional can be derived from the isotropic nearest-neighbor Heisenberg Hamiltonian H including the dipolar interaction¹ via the Kac-Hubbard-Stratonovich transformation,²⁰ where H is given by

$$\begin{aligned} H = & \int_{\vec{q}} U_q^{\alpha\beta} S_q^\alpha S_{-\vec{q}}^\beta, \\ U_q^{\alpha\beta} = & -J_0 \cdot \delta^{\alpha\beta} + J \left[q^2 a^2 \delta^{\alpha\beta} + g \frac{q^\alpha q^\beta}{q^2} \right]. \end{aligned} \quad (2)$$

Below T_c , \mathcal{F} is expanded to second order in the fluctuations $\delta\phi_q^\alpha$ about the order parameter, yielding

$$\begin{aligned} \mathcal{F}^{\text{tharm}} = & \sum_{q,\alpha\beta} \tilde{U}_q^{\alpha\beta} \delta\phi_q^\alpha \delta\phi_{-\vec{q}}^\beta, \\ \tilde{U}_q^{\alpha\beta} = & J \left[r_L \delta^{\alpha z} \delta^{\beta z} + q^2 \delta^{\alpha\beta} + g \frac{q^\alpha q^\beta}{q^2} \right], \\ r_L = & 1/\xi_-^2 \sim |T-T_c|. \end{aligned} \quad (3)$$

ξ_- (or ξ for short) is the correlation length below T_c . In mean-field theory, we have $\xi_+^2/\xi_-^2=2$ whereas including fluctuations one gets $\xi_+^2/\xi_-^2=4.08$. This ratio can be calculated from the corresponding homogeneous static susceptibilities according to

$$\frac{\xi_+}{\xi_-} = \left(\frac{\tilde{\chi}_0^+}{\tilde{\chi}_0^-} \right)^{1/(2-\eta)}. \quad (4)$$

Using the expression

$$\frac{\tilde{\chi}_0^+}{\tilde{\chi}_0^-} = \frac{\gamma}{\beta} \left[\frac{(1-2\beta)\gamma}{2\beta(\gamma-1)} \right]^{(\gamma-1)} \quad (5)$$

from Ref. 21, $\beta=0.375$ from Ref. 22, and $\gamma=1.375$ and $\eta=0.043$ from Ref. 23, this yields

$$\frac{\xi_+}{\xi_-} = 2.02. \quad (6)$$

To obtain the static susceptibility in mean-field approximation, we just have to invert the matrix \tilde{U}_q^- :

$$\chi_q^{\alpha\beta} = \frac{1}{2} (\tilde{U}_q^-)^{-1}{}^{\alpha\beta}. \quad (7)$$

This follows from using the partition function $Z_{\text{harm}} = e^{-\beta \int d[\delta\phi] \mathcal{F}^{\text{harm}}}$. Instead of q , ξ , and q_D we introduce scaling variables x , y and the corresponding polar coordinates R , ϕ according to

$$\begin{aligned} x = \frac{\sqrt{r_L}}{q} = \frac{1}{q\xi}, \quad y = \frac{\sqrt{g}}{q} = \frac{q_D}{q}, \\ R = \sqrt{x^2+y^2} = \frac{\sqrt{\xi^{-2}+q_D^2}}{q}, \quad \tan \phi = \frac{y}{x} = \sqrt{\frac{g}{r_L}} = q_D \xi. \end{aligned} \quad (8)$$

The variable ϕ is a measure for temperature while R accounts for the wave vector (at fixed temperature). Then, we can write down the eigenvalues l_i and eigenvectors \vec{v}_i of the susceptibility tensor, i.e.,

$$\chi_q^- \vec{v}_i = \frac{1}{2Jq^2 \cdot l_i} \vec{v}_i \quad (9)$$

in scaling form

$$\begin{aligned} l_1(R, \phi, \vartheta) = 1, \quad l_{2/3}(R, \phi, \vartheta) = 1 + R^2 \hat{F}_{-/+}(\vartheta, \phi), \\ \vec{v}_1(\vartheta, \phi) = \hat{p} \times \hat{e}_z, \quad \vec{v}_{2/3}(\vartheta, \phi) = \cos \varphi_{2/3}(\vartheta, \phi) \hat{p} \\ + \sin \varphi_{2/3}(\vartheta, \phi) \hat{e}_z, \end{aligned} \quad (10)$$

where we defined

$$\hat{F}_\pm(\vartheta, \phi) = \frac{1}{2} \{ 1 \pm \sqrt{1 - \sin^2 2\phi \cos^2 \vartheta} \}, \quad (11)$$

$$\varphi_3(\vartheta, \phi) = \varphi_2(\vartheta, \phi) + 90^\circ = \frac{1}{2} \arccos f(\vartheta, \phi) \in [0^\circ, 90^\circ],$$

$$\begin{aligned} f(\vartheta, \phi) = & \frac{\sin^2 \phi \cos 2\vartheta - \cos^2 \phi}{\sqrt{1 - \sin^2 2\phi \cos^2 \vartheta}} \\ = & \frac{2 \sin^2 \phi \cos^2 \vartheta - 1}{\sqrt{1 - \sin^2 2\phi \cos^2 \vartheta}}, \quad f(0^\circ, 45^\circ) = -1. \end{aligned} \quad (12)$$

Without loss of generality, we assume the magnetization to point along the z direction (defined by the unit vector \hat{e}_z). Basically, the unit vector \hat{p} is the projection of \vec{q} onto the

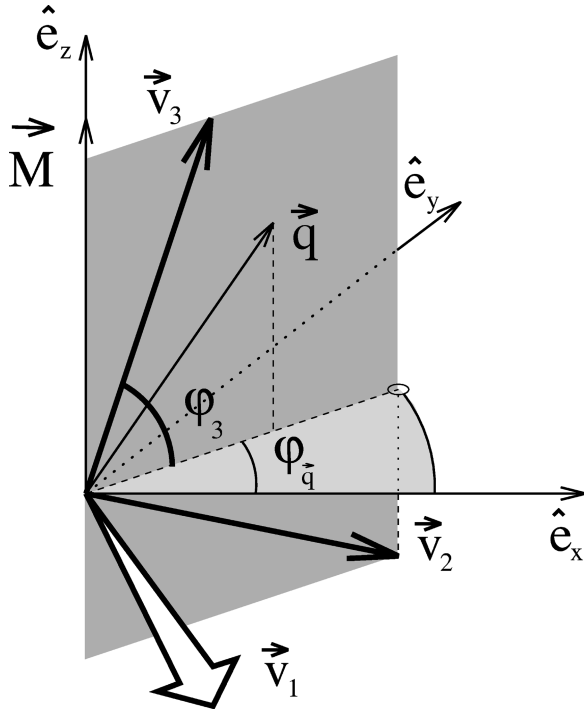


FIG. 1. Eigenvectors \vec{v}_i of the static susceptibility tensor. Vectors \hat{e}_z , \vec{M} , \vec{q} , \vec{v}_2 , and \vec{v}_3 all lie in the same plane, \vec{v}_1 is perpendicular to that plane.

x - y plane. The angle between the wave vector \vec{q} and the x - y plane $\vartheta \in [0^\circ, 90^\circ]$ and the vector \hat{p} are defined in the following way:

$$\vec{q} =: q \cdot \text{sgn } \vec{q} \cdot \begin{pmatrix} \cos \varphi \cos \vartheta \\ \sin \varphi \cos \vartheta \\ \sin \vartheta \end{pmatrix}, \quad (13)$$

$$\hat{p} = \begin{pmatrix} \cos \varphi \\ \sin \varphi \\ 0 \end{pmatrix} : = \begin{cases} \frac{\vec{e}_z \times (\vec{q} \times \vec{e}_z)}{p} \cdot \text{sgn } \vec{q} & \text{for } p := \sqrt{q_x^2 + q_y^2} \neq 0, \\ \vec{e}_y & \text{for } p = 0, \end{cases} \quad (14)$$

$$\text{sgn } \vec{q} := \begin{cases} \text{sgn } q_z, & q_z \neq 0, \\ \text{sgn } q_y, & q_z = 0, \quad q_y \neq 0, \\ \text{sgn } q_x, & q_z = q_y = 0, \quad q_x \neq 0, \\ 1, & q = 0. \end{cases} \quad (15)$$

With this choice of signs, the eigenvalues as well as the eigenvectors share the symmetry $l_i(-\vec{q}) = l_i(\vec{q})$, $\vec{v}_i(-\vec{q}) = \vec{v}_i(\vec{q})$ with the Hamiltonian. The functions \hat{F}_\pm have the following properties:

$$\hat{F}_+ + \hat{F}_- = 1, \quad \hat{F}_+ \geq \hat{F}_- \in [0, 1/2], \quad (16)$$

$$\hat{F}_\pm(\vartheta, 90^\circ - \phi) = \hat{F}_\pm(\vartheta, \phi).$$

As shown in Fig. 1 the eigenvectors define an orthonormal right-handed coordinate system. The one remaining Goldstone mode (eigenvalue l_1 and eigenvector \vec{v}_1) is perpendicular to \vec{q} and the magnetization \vec{M} . (It costs no energy to rotate \vec{M} around the direction of \vec{q} .) The other two modes lie in the plane defined by \vec{q} and \vec{M} , where \vec{v}_3 is rotated by an angle φ_3 out of the x - y plane (see Fig. 1). This direction is to be identified with the ‘‘longitudinal’’ mode since its eigenvalue l_3 is the largest of the l_i and becomes the inverse longitudinal susceptibility in the two limiting cases of isotropic exchange interaction only ($\phi = 0^\circ$) and at the Curie temperature $T = T_c$ ($\phi = 90^\circ$). In the vicinity of these two limiting cases, \vec{v}_3 is approximately parallel to the magnetization \vec{M} or the wave vector \vec{q} , respectively. Note, however, that the deviation from these directions as given by φ_3 in Eq. (12) can become as large as 45° . The border line between these two limiting cases is given by the condition

$$\tan \phi = 1. \quad (17)$$

For $\vec{q} \parallel \vec{M}$ ($\vartheta = 90^\circ$), the dipolar interaction enters only in the longitudinal mode and we regain two Goldstone modes perpendicular to \vec{M} . The longitudinal susceptibility has Ornstein-Zernicke form with an additional ‘‘mass’’ q_D^2 . As is evident from Eq. (10) the susceptibilities in the general case are described by expressions of Ornstein-Zernicke form with ‘‘anisotropic’’ (angle dependent) masses. A detailed discussion of the eigenvalues and hence the susceptibilities will be deferred to the next section, where fluctuations are included.

As a prerequisite for the next section, we restate the final results of this section, Eqs. (8)–(12), by introducing the quantities $\hat{r}_{(0)}^2(x, y) = x^2$, $\tilde{R}_{(0)}$, and $\tilde{\phi}_{(0)}$ according to

$$\tilde{R}_{(0)}(R, \phi) = \sqrt{\hat{r}_{(0)}^2(x, y) + y^2} = R, \quad (18)$$

$$\tan \tilde{\phi}_{(0)}(R, \phi) = y / \hat{r}_{(0)}(x, y) = \tan \phi$$

in the following form for the eigenvalues:

$$l_1(R, \phi, \vartheta) = 1, \quad l_{2/3}(R, \phi, \vartheta) = 1 + \tilde{R}_{(0)}^2 \hat{F}_{-/+}(\vartheta, R, \phi), \quad (19)$$

$$\hat{F}_\pm(\vartheta, R, \phi) = \frac{1}{2} \{ 1 \pm \sqrt{1 - \sin^2 2\tilde{\phi}_{(0)} \cos^2 \vartheta} \},$$

and the eigenvectors or eigendirections

$$\vec{v}_1(\vartheta, R, \phi) = \hat{p} \times \hat{e}_z,$$

$$\vec{v}_{2/3}(\vartheta, R, \phi) = \cos \varphi_{2/3}(\vartheta, R, \phi) \hat{p} + \sin \varphi_{2/3}(\vartheta, R, \phi) \hat{e}_z,$$

$$\varphi_3(\vartheta, R, \phi) = \varphi_2(\vartheta, R, \phi) + 90^\circ$$

$$= \frac{1}{2} \arccos f(\vartheta, R, \phi) \in [0^\circ, 90^\circ],$$

$$f(\vartheta, R, \phi) = \frac{\sin^2 \bar{\phi}_{(0)} \cos 2\vartheta - \cos^2 \bar{\phi}_{(0)}}{\sqrt{1 - \sin^2 2\bar{\phi}_{(0)} \cos^2 \vartheta}}, \quad (20)$$

$$f(0^\circ, R, 45^\circ) = -1.$$

III. MASS RENORMALIZATION

Now we include fluctuations in our considerations. Let us start with the isotropic ferromagnet. Below T_c , the transverse Goldstone modes have the pronounced effect of altering also the longitudinal susceptibility χ_L . Instead of being finite at all temperatures away from T_c as suggested by the mean field theory, χ_L actually diverges at all temperatures as $1/q$ with the wave vector. In Ref. 10 Mazenko has given an analytic expression for the longitudinal susceptibility of the isotropic Heisenberg model based on a reexponentiation procedure:

$$\begin{aligned} \hat{\chi}_L^{-1} &= 1 + x^2 \left\{ \frac{(n+8) + (5-n/2)\varepsilon}{9 + (n-1)x^\varepsilon} \right. \\ &\quad \left. - \frac{9\varepsilon}{n+8} \left[1 + \sqrt{1+4x^2} \ln \left(\frac{\sqrt{1+4x^2}-1}{2x} \right) \right] + O(\varepsilon^2) \right\} \\ &\approx 1 + x^2 \frac{29}{18+4x}. \end{aligned} \quad (21)$$

For the number of components we have $n=3$ and the separation from the upper critical dimension $d_c=4$ is $\varepsilon=d_c-d=1$. Although the derivation of Eq. (21) in Ref. 10 is not rigorous, a more sophisticated treatment yields essentially the same result.^{12,13} It is interesting to note that the asymptotic $1/q$ divergence shows up rather late (at very small q). Only at $x \approx 100$ does the effective exponent start to get close to -1 (see Fig. 2). Experimentally it is much more likely to detect the minimum in the effective exponent at $x \approx 3.3$ with a value of -1.4 for the effective exponent. Indeed, the $1/q$ singularity has not been observed up to now, while the associated $1/\sqrt{H}$ singularity has recently been detected.¹⁷

Now, our aim is to generalize the result (21) to the case including the dipolar interaction. There, due to the one Goldstone mode remaining, fluctuations will still influence the result. To this end, we take a look at the associated perturbation theory which has been developed by Täuber and Schwabl in Refs. 13, 19. This will tell us how to modify the mean-field results (18)–(20) in order to take account of the fluctuations. For details of the perturbation theory and for the analytic expressions we also refer the reader to Refs. 13, 19. We just present here the corresponding Feynman diagrams for the Cartesian components of the two-point-vertex function Γ , which in the static limit is proportional to the inverse susceptibility:

$$\begin{aligned} \Gamma^{\sigma\sigma} &= q^2 + m_0^2 - \text{diagram 1} - \text{diagram 2} - \text{diagram 3} \\ &\quad - \text{diagram 4} - \text{diagram 5} - \text{diagram 6} \\ \Gamma^{\sigma\pi^\alpha} &= g_0 P_L^{\alpha n} - \text{diagram 7} - \text{diagram 8} - \text{diagram 9} \\ \Gamma^{\pi^\alpha\pi^\beta} &= q^2 P_T^{\alpha\beta} + (g_0 + q^2) P_L^{\alpha\beta} - \text{diagram 10} - \text{diagram 11} \\ &\quad - \text{diagram 12} - \text{diagram 13} - \text{diagram 14} \end{aligned} \quad (22)$$

The indices α, β refer to the $n-1$ transverse components (π^α), while σ is the n th, longitudinal component. The quantity m_0 is proportional to the order parameter, and g_0 again measures the strength of the dipolar interaction. Finally, we introduced the projectors $P_L^{\alpha\beta} = q^\alpha q^\beta / q^2$, and $P_T = \mathbf{1}_n - P_L$, where $\mathbf{1}_n$ is the $n \times n$ unity matrix. Leaving out the diagrams (or setting $\varepsilon=0$), we just recover the mean field results, which can equivalently be stated as in Eqs. (18)–(20).

Since we are interested in critical phenomena, we study the coexistence limit ($q \rightarrow 0$). In this limit, it can be shown¹⁹ that to leading one loop order only the expression for $\Gamma^{\sigma\sigma}$ is modified by the fluctuations while all the other diagrams cancel or are of higher order:

$$\Gamma^{\sigma\sigma} = q^2 + m_0^2 - \text{diagram 15}, \quad (23)$$

where the propagator is given by

$$\frac{\pi}{q^2} = \frac{1}{q^2} \bar{P}_T^{\alpha\beta} + \frac{1}{q^2 + g_0 \cos^2 \vartheta} \bar{P}_L^{\alpha\beta}. \quad (24)$$

Here, we defined the $(n-1) \times (n-1)$ matrices $\bar{P}_L = P_L [q^2 / (q^2 - q_n^2)]$ and $\bar{P}_T = \mathbf{1}_{n-1} - \bar{P}_L$. This result amounts simply to a modification of the wave-vector dependence through the renormalized mass term. Thus, in order to get an expression for the susceptibility including fluctuations, we only have to insert a renormalized mass into the formulas (18)–(20) for the susceptibility. In the case of the isotropic limit this expression was reexponentiated¹⁰ to obtain Eq. (21). The mean field result m_0^2 is replaced by

$$m_0^2 - \text{diagram 16}$$

where now, the propagator has the form ($g_0=0$)

$$\frac{\pi}{q^2} = \frac{1}{q^2} \mathbf{1}_{n-1}. \quad (25)$$

In scaling variables, this yields a replacement of $\hat{r}_{(0)}^2(x, 0) = x^2$ by

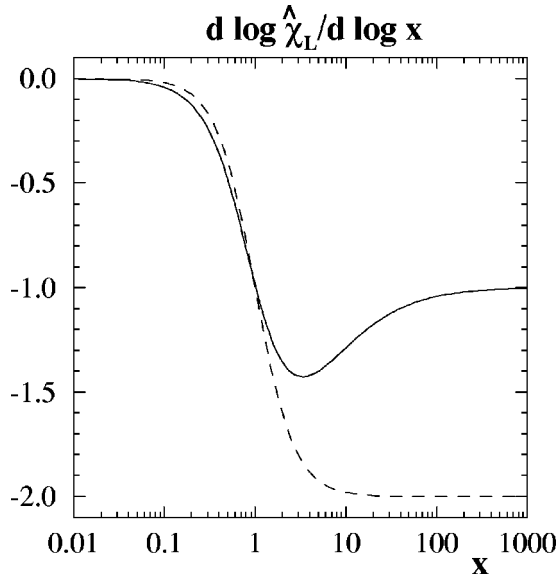


FIG. 2. Effective exponent of the longitudinal static susceptibility $d \log \hat{\chi}_L / d \log x$ vs scaling variable $x = 1/q\xi$. Solid: Eq. (21); dashed: Result of the mean-field theory (Ornstein-Zernike).

$$\begin{aligned} \hat{r}^2(x,0) &= x^2 \left\{ \frac{(n+8) + (5-n/2)\varepsilon}{9+x^\varepsilon[n-1]} \right. \\ &\quad \left. - \frac{9\varepsilon}{n+8} \left[1 + \sqrt{1+4x^2} \ln \left(\frac{\sqrt{1+4x^2}-1}{2x} \right) \right] \right. \\ &\quad \left. + O(\varepsilon^2) \right\} \\ &= \frac{29x^2}{18+4x} - \frac{9x^2}{11} \left[1 + \sqrt{1+4x^2} \ln \left(\frac{\sqrt{1+4x^2}-1}{2x} \right) \right] \\ &\quad + O(\varepsilon^2) \end{aligned} \tag{26}$$

in Eqs. (18)–(20). This leads to the expression (21) for the longitudinal susceptibility χ_L .

To obtain the result in the general case, i.e. for arbitrary wave number, we would have to evaluate the diagram in Eq. (23) for $g_0 \neq 0$. For the extreme dipolar limit, we get the same result as for the isotropic limit except for a factor of $(n-1)/(n-2) = 2$.¹⁹ This factor stems from the reduction of the number of the Goldstone modes by one in the presence of the dipolar interaction.¹⁹ In scaling variables this amounts to

$$\begin{aligned} \hat{r}^2(x,\infty) &= x^2 \left\{ \frac{(n+8) + (5-n/2)\varepsilon}{9+x^\varepsilon[n-2]} \right. \\ &\quad \left. - \frac{9\varepsilon}{n+8} \left[1 + \sqrt{1+4x^2} \ln \left(\frac{\sqrt{1+4x^2}-1}{2x} \right) \right] \right. \\ &\quad \left. + O(\varepsilon^2) \right\} \\ &= \frac{29x^2}{18+2x} - \frac{9x^2}{11} \left[1 + \sqrt{1+4x^2} \ln \left(\frac{\sqrt{1+4x^2}-1}{2x} \right) \right] \\ &\quad + O(\varepsilon^2). \end{aligned} \tag{27}$$

Setting $g_0 \rightarrow \infty$, the propagator in Eq. (23) may be written as

$$\pi = \frac{1}{q^2} \bar{P}_T^{\alpha\beta}. \tag{28}$$

For the general case, i.e. for arbitrary wave number, we note that in dimensional regularization the evaluation of the diagram in Eq. (23) yields results of $(n-1)q^{-\varepsilon}$ and $(n-2)q^{-\varepsilon}$ for the isotropic and dipolar limit, respectively.¹⁹ Due to its angular dependency, the propagator (24) is extremely complicated in the general case and it would be very cumbersome to evaluate the diagram exactly. Instead, we propose to interpolate its value according to Table I.

In scaling variables, this amounts to using

$$\begin{aligned} \hat{r}^2(x,y) &= x^2 \left\{ \frac{(n+8) + (5-n/2)\varepsilon}{9+x^\varepsilon[(n-2) + (1+y^2)^{-\varepsilon/2}]} \right. \\ &\quad \left. - \frac{9\varepsilon}{n+8} \left[1 + \sqrt{1+4x^2} \ln \left(\frac{\sqrt{1+4x^2}-1}{2x} \right) \right] \right. \\ &\quad \left. + O(\varepsilon^2) \right\} \\ &= \frac{29x^2}{18+2x[1+(1+y^2)^{-1/2}]} - \frac{9x^2}{11} \\ &\quad \times \left[1 + \sqrt{1+4x^2} \ln \left(\frac{\sqrt{1+4x^2}-1}{2x} \right) \right] + O(\varepsilon^2) \end{aligned} \tag{29}$$

TABLE I. Values of the diagram for the mass renormalization in the isotropic ($g_0=0$) and dipolar limit ($g_0=\infty$) and in the general case.

Propagator		Value of the diagram
$g_0=0$	$\frac{\pi}{q^2} \mathbf{1}_{n-1}$	$\sigma^+ \circlearrowleft_{\pi} \sigma^+ \sim (n-1) q^{-\varepsilon}$
$g_0=\infty$	$\frac{\pi}{q^2} \bar{P}_T^{\alpha\beta}$	$\sigma^+ \circlearrowleft_{\pi} \sigma^+ \sim (n-2) q^{-\varepsilon}$
g_0	$\frac{\pi}{q^2} \bar{P}_T^{\alpha\beta} + \frac{1}{q^2 + g_0 \cos^2 \vartheta} \bar{P}_L^{\alpha\beta}$	$\sigma^+ \circlearrowleft_{\pi} \sigma^+ \sim (n-2) q^{-\varepsilon} + (q^2 + g_0)^{-\varepsilon/2}$

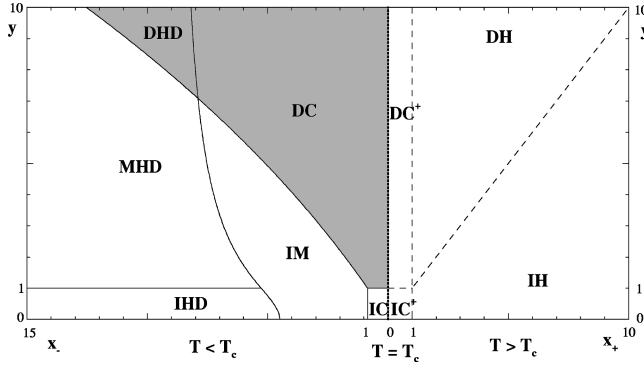


FIG. 3. Six characteristic regions for the static susceptibility below T_c in the x - y plane. (See text for the abbreviations.) Shaded: Dipolar dominated regions below T_c . Dashed: Borders of the corresponding regions above T_c .

for the Goldstone-mode renormalized mass, instead of its unrenormalized counterpart $\hat{r}_{(0)}^2(x, y) = x^2$. Analogously to Ref. 10, a reexponentiation procedure is employed to obtain these results.

This result is only an approximation. For example, we neglected possible angular dependencies in the average over the $n-2$ Goldstone modes and the one ‘‘dipolar mode.’’ But since this simplification only affects the precise form of the crossover while the limiting cases are correctly implemented (we have to say more about that), we believe that this expression will reproduce correctly the essential physical properties in a qualitative way. Anyhow, even if it were possible to calculate the diagram exactly, the remaining uncertainty introduced by the reexponentiation procedure is hard to overcome. To improve this procedure would be very cumbersome—if feasible at all. Thus from Eqs. (18)–(20) we end up with the final formulas for the scaling functions l_i of the static susceptibilities $\chi_q^i = 1/2Jq^2l_i$:

$$l_1(R, \vartheta, \phi) = 1, \quad l_{2/3}(R, \phi, \vartheta) = 1 + \bar{R}^2 \hat{F}_{-/ +}(\vartheta, R, \phi), \quad (30)$$

$$\hat{F}_{\pm}(\vartheta, R, \phi) = \frac{1}{2} \{1 \pm \sqrt{1 - \sin^2 2\bar{\phi} \cos^2 \vartheta}\}.$$

Here, we introduced the new scaling functions \bar{R} and $\bar{\phi}$:

$$\bar{R}(R, \phi) = \sqrt{\hat{r}^2(x, y) + y^2}, \quad \tan \bar{\phi}(R, \phi) = y/\hat{r}(x, y), \quad (31)$$

instead of $\bar{R}_{(0)} = R$ and $\bar{\phi}_{(0)} = \phi$ in Eq. (18). The corresponding directions or eigenvectors are given by

$$\vec{v}_1(\vartheta, R, \phi) = \hat{p} \times \hat{e}_z,$$

$$v_{2/3}(\vartheta, R, \phi) = \cos \varphi_{2/3}(\vartheta, R, \phi) p + \sin \varphi_{2/3}(\vartheta, R, \phi) e_z,$$

$$\varphi_3(\vartheta, R, \phi) = \varphi_2(\vartheta, R, \phi) + 90^\circ = \frac{1}{2} \arccos f(\vartheta, R, \phi) \in [0^\circ, 90^\circ],$$

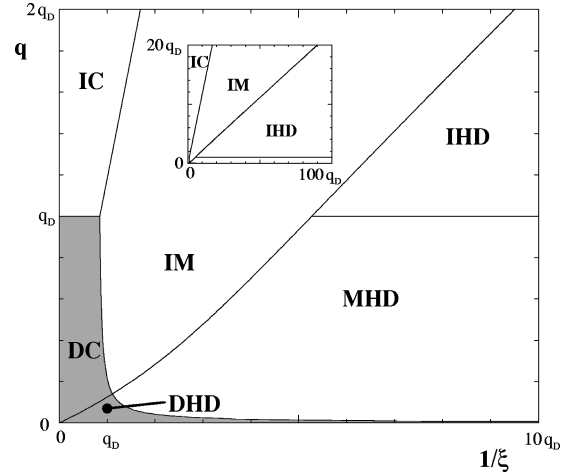


FIG. 4. Six characteristic regions for the static susceptibility below T_c in the κ_1 - κ_2 plane ($\kappa_1 = 1_D \xi$, $\kappa_2 = q/q_D$). Shaded: Dipolar dominated regions. Inset: The remaining three regions in the case of very weak dipolar interaction.

$$f(\vartheta, R, \phi) = \frac{\sin^2 \bar{\phi} \cos 2\vartheta - \cos^2 \bar{\phi}}{\sqrt{1 - \sin^2 2\bar{\phi} \cos^2 \vartheta}}, \quad (32)$$

$$f(0^\circ, R, \phi) = -1 \quad (R, \phi \text{ such that } \bar{\phi} = 45^\circ).$$

IV. DISCUSSION

In order to better understand the results (30)–(32) we discuss several limiting cases. To this end we neglect the numerically unimportant second term involving the logarithm in Eq. (29). The border line for the eigenvectors between approximately parallel to the magnetization \vec{M} and approximately parallel to \vec{q} is given by [cf. Eq. (17)]

$$\tan \bar{\phi} = 1. \quad (33)$$

In terms of x and y this is a line determined by

$$x = f_1(y) := \frac{y^2 [1 + (1 + y^2)^{-1/2}]}{29} + \sqrt{\frac{y^4 [1 + (1 + y^2)^{-1/2}]^2}{29^2} + \frac{18y^2}{29}}. \quad (34)$$

Below, we will define regions in the x - y plane, corresponding to these limiting cases and we will denote them with I (for isotropic), M (for the intermediate or crossover region) if $\tan \bar{\phi} < 1$, or D (for dipolar) if $\tan \bar{\phi} > 1$.

The eigenvalues or susceptibilities behave qualitatively different, depending on the demoninator of the first term in Eq. (29). Two cases can be identified, separated by the line

$$x = f_2(y) := \frac{9}{[1 + (1 + y^2)^{-1/2}]}. \quad (35)$$

For $x < f_2(y)$ we have $\hat{r}^2 \sim x^2$, which amounts to a ‘‘critical’’ or Ornstein-Zernike-like behavior for the susceptibility. Thus, we use C (for critical) or M (again for intermediate or crossover region) in this case. The other case is characterized

TABLE II. Leading order of the static susceptibilities in the six different regions defined in the main text.

Region	χ_1 ($\perp \vec{q}, \vec{M}$)	χ_2 (\perp EV)	for $\vec{q} \perp \vec{M}$	for $\vec{q} \parallel \vec{M}$	χ_3 (\parallel EV)	EV
IC	$\frac{1}{2Jq^2}$	$\frac{1}{2Jq^2}$			$\frac{1}{2Jq^2}$	\vec{M}
IM	$\frac{1}{2Jq^2}$	$\frac{1}{2J(q^2+q_D^2 \cos^2 \vartheta)}$	$\frac{1}{2J(q^2+q_D^2)}$	$\frac{1}{2Jq^2}$	$\frac{1}{2J[q^2+(29/18)\xi^{-2}]}$	\vec{M}
IHD	$\frac{1}{2Jq^2}$	$\frac{1}{2Jq^2}$			$\frac{1}{(29/2)Jq\xi^{-1}}$	\vec{M}
MHD	$\frac{1}{2Jq^2}$	$\frac{1}{2J(q^2+q_D^2 \cos^2 \vartheta)}$	$\frac{1}{2Jq_D^2}$	$\frac{1}{2Jq^2}$	$\frac{1}{29Jq\xi^{-1}}$	\vec{M}
DHD	$\frac{1}{2Jq^2}$	$\frac{1}{2J[q^2+(29/2)q\xi^{-1} \cos^2 \vartheta]}$	$\frac{1}{29Jq\xi^{-1}}$	$\frac{1}{2Jq^2}$	$\frac{1}{2Jq_D^2}$	\vec{q}
DC	$\frac{1}{2Jq^2}$	$\frac{1}{2J[q^2+(29/18)\xi^{-2} \cos^2 \vartheta]}$	$\frac{1}{2J[q^2+(29/18)\xi^{-2}]}$	$\frac{1}{2Jq^2}$	$\frac{1}{2J(q^2+q_D^2)}$	\vec{q}

by $\hat{r}^2 \sim x$ which leads to the $1/q$ singularity. Therefore, we have chosen the abbreviation HD (for hydrodynamic) in this case.

Finally, we get a third line defined by

$$y = 1, \quad (36)$$

separating regions where the susceptibility is more dipolar or more isotropic. Altogether, we have therefore six regions in the x - y plane, where the static susceptibilities show qualitatively different behavior. These regions are shown in Fig. 3.

Also included are the corresponding four regions above T_c as defined in Ref. 24. Note that we use different scaling variables x_+ and x_- above and below T_c , respectively. This corresponds to the distinction between ξ_+ and ξ_- .

In the Appendix we gathered the analytic expressions for the leading dependencies of the three susceptibilities in all six cases. Obviously, the results above (see Ref. 4) and below T_c join continuously at T_c ($x=0$). In the isotropic case ($y=0$) our result reproduces the expression given by Mazenko.¹⁰ This expression has basically been confirmed by sophisticated renormalization group calculations in Refs. 12, 13. Furthermore, our result is also in accord with renormalization group calculations in the so-called coexistence limit including dipolar interactions¹⁹ (where the wave vector q vanishes and we reach the extreme dipolar region). In particular this holds for the reduction factor of 2 (for $n=3$ component magnets) by which the longitudinal susceptibility is reduced in the dipolar region. This result corresponds to the disappearance of one Goldstone mode, leaving only one in the dipolar case. In this case as in all other limiting cases the longitudinal susceptibility is to leading order isotropic (does not depend on the angle between magnetization \vec{M} and wave vector \vec{q}). This is also true exactly of course for the remaining Goldstone mode, while the second ‘‘transverse’’ mode does show an angular dependence. Due to the dipolar interaction fluctuations are reduced (there is an additional ‘‘mass term’’ in the theory). Accordingly, the susceptibilities are reduced compared to the isotropic case. Nevertheless, the longitudinal susceptibility still diverges (with a smaller am-

plitude, however). In the ultimate limit of vanishing wave vector, it is finite due to demagnetization effects. The second transverse susceptibility (which in the isotropic case corresponds to a Goldstone mode) also still diverges but has a smaller exponent. Instead of $\sim q^{-2}$ the leading asymptotics is $\sim q^{-1}$.

To facilitate the comparison between experiment and theory, we also include the same diagram in the physically more transparent variables $\kappa_1 = x/y = 1/q_D \xi$ and $\kappa_2 = 1/y = q/q_D$, i.e., essentially in the temperature–wave-vector plane ($1/\xi$ q plane). We therefore measure these quantities in units of the dipolar wave vector q_D (see Fig. 4).

In the inset of Fig. 4 we show the corresponding diagram for very small q_D , i.e., for negligible dipolar interaction.

In these units we get the expected result that dipolar effects become important in the vicinity of T_c and also for vanishing q . The region DC is reached when q and $1/\xi$ are smaller than q_D which was to be expected. To enter region DHD , however, q quite unexpectedly has to be small compared to one tenth of q_D or even less.

V. SUMMARY

To summarize, we have derived analytic expressions for the static susceptibilities of the isotropic Heisenberg ferromagnet below T_c including the dipolar interaction and including fluctuations induced by the Goldstone modes [Eqs. (30)–(32)]. Special emphasis was put on the necessity to discuss eigenvalues and eigenvectors of the susceptibility tensor. It has been shown again that the number of Goldstone modes is reduced from 2 to 1 due to the dipolar interaction, which leads among other effects to a reduction of the amplitude of the divergent longitudinal susceptibility by a factor of 2. While one of the transverse susceptibilities—belonging to the one Goldstone mode remaining—stays unaltered, the other one still diverges, but less rapidly being $\sim 1/q$ instead of $\sim 1/q^2$ in the isotropic limit. Although the magnitudes of the susceptibilities are generally reduced (because fluctuations are diminished) due to the additional mass introduced by the dipolar interaction, the longitudinal susceptibility still

diverges $\sim 1/q$ as the wave vector q approaches 0, until it enters the region where demagnetization effects become important which keep the susceptibility finite. This $1/q$ divergence is very hard to see experimentally because it shows up only at very tiny values of $q\xi$ (ξ is the correlation length). It seems more promising to search for the minimum in the effective exponent (cf. Fig. 2). Finally, in the Appendix, we presented expressions for the susceptibilities to leading order in six characteristic regions in the temperature–wave-vector plane. The dipolar dominated region near T_c (the inverse correlation length there has to be smaller than the dipolar wave vector q_D) is reached if the wave vector is small compared to q_D . Unexpectedly, the asymptotic dipolar region far from T_c can be reached only for wave vectors smaller than a tenth of q_D or even less (cf. Fig. 4).

ACKNOWLEDGMENTS

It is a pleasure to thank U. C. Täuber and E. Frey for valuable and helpful discussions. This work was supported by the German Federal Ministry for Research and Technology (BMFT) under Contract Nos. 03-SC3TUM and 03-SC4TUM2.

APPENDIX

In this appendix we summarize the analytic results for the leading dependencies of the static susceptibilities in the six different regions defined in the main text. The longitudinal susceptibility χ_3 is to leading order independent of the angle ϑ . The corresponding eigendirection is approximately parallel to the magnetization \vec{M} or, in the dipolar dominated regions, to the wave vector \vec{q} . [Note, however, that the deviation from these directions, given by the angle φ_3 in Eq. (32) can be quite substantial.] The two cases are indicated by the symbol \vec{M} or \vec{q} , respectively, in the column EV of Table II. The one remaining Goldstone-mode dominated susceptibility χ_1 is always independent of ϑ . Its corresponding eigenvector is perpendicular to both \vec{M} and \vec{q} . The second transverse mode does depend on ϑ even to leading order. In this case we have therefore also given the results for the two interesting special cases, $\vartheta=0^\circ$, i.e., $\vec{q}\perp\vec{M}$, and $\vartheta=90^\circ$, i.e., $\vec{q}\parallel\vec{M}$. The corresponding eigenvector is perpendicular to the other two eigendirections, i.e., approximately perpendicular to either \vec{M} or \vec{q} .

-
- ¹M. E. Fisher and A. Aharony, Phys. Rev. Lett. **30**, 559 (1973); Phys. Rev. B **8**, 3323 (1973); A. Aharony, *ibid.* **8**, 3342 (1973).
²A. Aharony, in *Phase Transitions and Critical Phenomena*, edited by C. Domb and M. S. Green (Academic, New York, 1976), Vol. 6, and references therein.
³A. D. Bruce and A. Aharony, Phys. Rev. B **10**, 2078 (1974); **10**, 2973 (1974); T. Nattermann and S. Trimper, J. Phys. C **9**, 2589 (1976); A. D. Bruce, J. M. Kosterlitz, and D. R. Nelson, *ibid.* **9**, 825 (1976); A. D. Bruce, *ibid.* **10**, 419 (1977); M. A. Santos, *ibid.* **13**, 1205 (1980); H. S. Kogon and A. D. Bruce, *ibid.* **15**, 5729 (1982).
⁴E. Frey and F. Schwabl, Phys. Rev. B **43**, 833 (1991).
⁵M. E. Fisher and A. Aharony, Phys. Rev. B **10**, 2818 (1974).
⁶N. D. Mermin and H. Wagner, Phys. Rev. Lett. **17**, 1133 (1966); P. C. Hohenberg, Phys. Rev. **158**, 383 (1967).
⁷H. Mori and K. Kawasaki, Prog. Theor. Phys. **27**, 529 (1962); **28**, 690 (1962).
⁸F. Schwabl and K. H. Michel, Phys. Rev. B **2**, 189 (1970).
⁹E. Brézin and D. J. Wallace, Phys. Rev. B **7**, 1967 (1973); D. R. Nelson, *ibid.* **13**, 2222 (1976); E. Brézin and J. Zinn-Justin, *ibid.* **14**, 3110 (1976).
¹⁰G. F. Mazenko, Phys. Rev. B **14**, 3933 (1976).
¹¹A. Z. Patashinskii and V. L. Pokrovskii, Sov. Phys. JETP **37**, 733 (1973); V. L. Pokrovsky, Adv. Phys. **28**, 595 (1979).
¹²I. D. Lawrie, J. Phys. A **14**, 2489 (1981); **18**, 1141 (1985).
¹³U. C. Täuber and F. Schwabl, Phys. Rev. B **46**, 3337 (1992).
¹⁴H. S. Toh and G. A. Gehring, J. Phys.: Condens. Matter **2**, 7511 (1990).
¹⁵S. W. Lovesey and K. N. Trohidou, J. Phys.: Condens. Matter **3**, 1827 (1991); **3**, 5255(E) (1991); A. Cuccoli, S. W. Lovesey, G. Pedrolli, and V. Tognetti, *ibid.* **5**, 3241 (1993).
¹⁶T. Holstein and H. Primakoff, Phys. Rev. **58**, 1098 (1940).
¹⁷J. Kötzler, D. Görlitz, R. Dombrowski, and M. Pieper, Z. Phys. B **94**, 9 (1994).
¹⁸H. Schinz and F. Schwabl, following paper, Phys. Rev. B **57**, 8438 (1998).
¹⁹U. C. Täuber and F. Schwabl, Phys. Rev. B **48**, 186 (1993).
²⁰D. J. Amit, *Field Theory, the Renormalization Group, and Critical Phenomena*, 2nd ed. (World Scientific, Singapore, 1984).
²¹P. Schofield, J. D. Litster, and J. T. Ho, Phys. Rev. Lett. **23**, 1098 (1969).
²²R. L. Stephenson and P. J. Wood, J. Phys. C **3**, 90 (1970).
²³D. S. Ritchie and M. E. Fisher, Phys. Rev. **5**, 2668 (1972).
²⁴E. Frey and F. Schwabl, Z. Phys. B **71**, 355 (1988); **76**, 139(E) (1989).